Atmospheric Environment 202 (2019) 8–16

Contents lists available at ScienceDirect

Atmospheric Environment

journal homepage: www.elsevier.com/locate/atmosenv

Evaluation of MAIAC aerosol retrievals over China

Zhaoyang Zhang[a,*], Weiling Wu[b], Meng Fan[c], Jing Wei[d], Yunhui Tan[a], Quan Wang[e,**]

[a] College of Geography and Environmental Sciences, Zhejiang Normal University, Zhejiang Province, China
[b] Chinese Academy for Environmental Planning, Beijing, China
[c] State Key Laboratory of Remote Sensing Science, Institute of Remote Sensing and Digital Earth, Chinese Academy of Sciences, Beijing, China
[d] State Key Laboratory of Remote Sensing Science, College of Global Change and Earth System Science, Beijing Normal University, Beijing, China
[e] Faculty of Agriculture, Shizuoka University, Shizuoka, Japan

ARTICLE INFO

Keywords:
Aerosol optical depth
Validation
AERONET
MAIAC

ABSTRACT

Multiangle Implementation of Atmospheric Correction (MAIAC) is a new aerosol algorithm developed to retrieve aerosol optical depth (AOD) over land using the time series data to dynamically isolate aerosol and land contributions. However, there are still no comprehensive research on the quality of MAIAC AOD over China. In this paper, 1 km MAIAC AOD over China were examined against ground-based measurements to evaluate the performance of the data. In general, Aqua and Terra MAIAC retrievals have a high correlation coefficient (0.924 for Aqua and 0.933 for Terra) with ground-based observations and there are more than 72% of retrievals falling within the Expected Errors (EE = ± (0.05 + 0.2*AOD)). We found that the accuracy of MAIAC AOD is related with the AOD magnitude, aerosol size, seasons and surface types. In spring and summer, the AOD bias was influenced by both aerosol model and surface reflectance estimation. We also found that the aerosol model is the main source of AOD bias over desert regions. These results indicated that the MAIAC AOD could be used as a new aerosol data source for air quality and climate studies in China.

1. Introduction

Aerosols are defined as the suspended particles in the atmosphere, which contains various of particles having different compositions, shapes, sizes and optical properties (Hinds, 1999). Aerosols can absorb and scatter the solar radiation to cool the surface and heat up atmosphere (Malm et al., 1996; Zhong et al., 2016). Aerosol affecting the global radiative budget is still one of the largest uncertainties in climate research (Field et al., 2014). Therefore, the comprehensive analysis of atmospheric aerosols is essential to the climate changes studies (Ramanathan and Feng, 2009; Yassaa, 2016).

Aerosol optical properties can be provided by the ground-based instruments, such as sun photometer and lidar. However, the ground-based instruments cannot characterize the regional aerosol properties with enough spatial resolutions for climate change studies due to the limited number of the surface stations. Satellite sensors observe atmospheric information from space and can be used to retrieve the regional aerosol properties (Zhang et al., 2016b). Aerosol optical depth (AOD) is one of the fundamental aerosol optical properties that can quantify the amount of aerosol loadings (Zhang et al., 2016a, 2017). In recent years, the aerosol algorithm for satellite has been improved a lot and the satellite AOD was adopted to do some research in air quality, regional climate change, and human health (Wang et al., 2010; Zhuang et al., 2013; Li et al., 2016; Zhang and Wong, 2017). Although the satellite aerosol retrievals have large improvements, there are still many uncertainties in satellite aerosol datasets (Tao et al., 2017).

Aerosol data sets from MODerate Imaging Spectrometer (MODIS) are the most commonly used aerosol products (Ghotbi et al., 2016; Lin et al., 2016; Li et al., 2017). There are two MODIS sensors monitoring the Earth from the space, including Terra (launched February 2000) and Aqua (launched June 2002) (Ichoku et al., 2004). MODIS sensors retrieve land aerosol information using Dark Target (DT) and Deep Blue (DB) algorithms (Levy et al., 2010; Hsu et al., 2013). DT algorithm separates aerosol and land contribution by establishing the empirical relationship of surface reflectance between visible and shortwave infrared bands. This algorithm is very effective for retrieving AOD over dense vegetation areas. DB algorithm is developed to retrieve the AOD over bright surface using pre-calculated surface database. MODIS aerosol algorithm has been updated to Version 6.1 to retrieve accurate and high-quality aerosol products (Tao et al., 2015, 2017; Zhang et al., 2016b; Levy et al., 2018; Wei et al., 2018). However, there are still some uncertainties in MODIS aerosol products, such as bidirectional

* Corresponding author.
** Corresponding author.
E-mail addresses: zhzhyang@outlook.com (Z. Zhang), wang.quan@shizuoka.ac.jp (Q. Wang).

https://doi.org/10.1016/j.atmosenv.2019.01.013
Received 12 September 2018; Received in revised form 7 January 2019; Accepted 9 January 2019
Available online 14 January 2019
1352-2310/

reflectance factor and the merged DT and DB data sets. Multiangle Implementation of Atmospheric Correction (MAIAC) is a recent aerosol algorithm developed to retrieve AOD over land (Lyapustin et al., 2011a, 2011b, 2012). The algorithm adopts the time series data to dynamically separate aerosol and land contributions. The advantage of the algorithm is that it can retrieve AOD over both dense vegetation regions and bright surface and it also considers the BRDF effects (Lyapustin et al., 2018). Martins et al. (2017) and Superczynski et al. (2017) estimated the MAIAC data accuracy over South America and North America. These results suggested that MAIAC performed well over these regions. The data can be used to derive the high-resolution surface particle matter concentrations. However, the data is still not fully validated over China. This is vital to consolidate the confidence in aerosol products and their applications.

China experienced severe aerosol pollution in recent years (Zhang et al., 2015, 2018). The pollution is formed by both natural and artificial process. The complicated situation could induce large errors in aerosol measurements. The widespread haze might be misclassified as cloud and screened from MODIS aerosol products (Li et al., 2009; Tao et al., 2017; Zhang et al., 2019b). The problem was improved in MODIS version 6 DB aerosol product. However, there are still large differences between DT and DB AOD under high AOD (Tao et al., 2015). It is critical to observe the real situation of atmospheric aerosol (Zhang et al., 2017, 2019a). MAIAC aerosol products might be one of the options to better understand the aerosol information over China. This also needs a comprehensive evaluation on MAIAC AOD.

In this study, a comprehensive study about MAIAC AOD is conducted over China using ground-based observations. The purpose in this paper is to investigate the influence factors on MAIAC aerosol retrievals in different situations and to examine the performance of MAIAC AOD over China. The paper is organized as follows: descriptions of the data are outlined in Section 2. Section 3 shows the evaluation method. MAIAC and AERONET AOD comparison are presented in Section 4. Section 5 discusses the results in this paper. Section 6 summarizes the major findings and conclusions.

2. Data sets

2.1. MAIAC AOD

MAIAC AOD are available for Aqua and Terra through NCCS ftp portal (ftp://maiac@dataportal.nccs.nasa.gov/DataRelease). The daily MAIAC AOD at 550 nm from 2002 to 2017 is at a spatial resolution of 1 km. The MAIAC algorithm decouples aerosol and surface contributions using the time series data. The algorithm assumes that the surface is stable over a short time and heterogeneous spatially. The algorithm considers the effects of bidirectional surface reflectance. MAIAC algorithm uses background aerosol models and SHARM scalar code to create look up table. Validation over South America and North America shows that the MAIAC AOD has better accuracy than DT retrievals over dense vegetation areas and generally improves accuracy of DB measurements over bright regions (Martins et al., 2017; Superczynski et al., 2017). To evaluate the accuracy of MAIAC AOD, the expected error (EE) envelopes is defined as ± (0.05 + 0.2*AOD) over land (Remer et al., 2013). The validation analysis also uses the root-mean-square error (RMSE) and correlation coefficient to evaluate the accuracy of MAIAC AOD.

2.2. AERONET

To reconcile satellite-based dataset, ground-based AOD measurements collected using sun-photometer in the AErosol RObotic NETwork (AERONET; (Holben et al., 1998)) are considered. In this paper, 16 selected AERONET stations are mapped in Fig. 1. AERONET AOD data have higher accuracy of < ± 0.01 for retrieval at wavelengths longer than 440 nm and < ± 0.02 for shorter wavelengths without cloud contamination (Holben et al., 1998). AERONET AOD bias can reach at

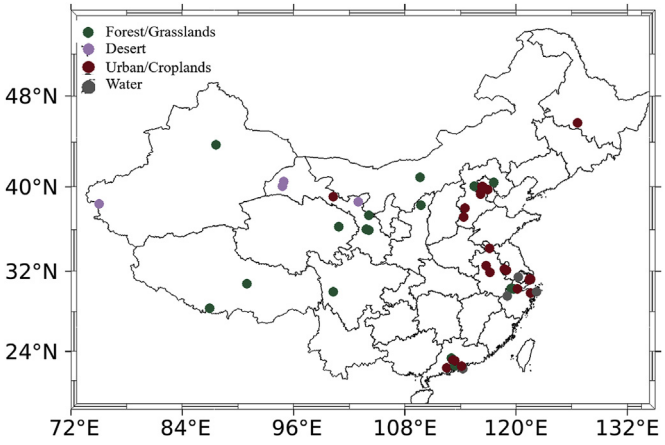

Fig. 1. Map of the selected AERONET station and land cover.

0.031–0.060 due to thin cirrus cloud contamination (Chew et al., 2011). These data become an important regional context to ensure representativeness of the satellite data. In order to evaluate the accuracy of MAIAC AOD, AERONET level 1.5 version 3 AOD data were used if level 2 AOD is not available for particular site in this paper. The MAIAC AOD is at 550 nm and the AERONET AOD at 550 nm is calculated using Ångström exponent and AOD in 670 nm and 440 nm (Tao et al., 2015). The SONET is a ground-based Cimel radiometer network with the extension of multiwavelength polarization measurement capability to observe long-term columnar atmospheric aerosol properties over China (Li et al., 2018). Table 1 shows the specific locations and land cover of each AERONET site in mainland of China. The land cover for the ground-based station is adopted from the MODIS Land Cover and Land Cover Dynamics product (MCD12C1) (Friedl et al., 2002).

3. Evaluation method

To evaluate the performance of MAIAC AOD, the assessment is based on three statistical parameters namely: Correlation Coefficient (R), Root Mean Square Error (RMSE) and expected error. The correlation coefficient is calculated by using linear regression. RMSE can obtained by following equations:

$$\mathrm{RMSE} = \sqrt{\frac{1}{n}\sum_{i=1}^{n}(AOD_{(AERONET)i} - AOD_{(MAIAC)i})^2}$$

where $AOT_{(AERONET)i}$ is the aerosol measurements from ground-based stations and $AOT_{(MAIAC)i}$) is the MAIAC AOD from the corresponding spatial and temporal windows. n is the total number of collocated satellite and ground-based measurements. Aerosol model and surface reflectance are the two important factors that influence the accuracy of aerosol algorithm. The slope of linear regression can represent the uncertainties induced by surface reflectance (Levy et al., 2010; Tao et al., 2015). The expected errors of DT AOD are within ± 0.05 ± 0.2*$\mathrm{AOD}_{\mathrm{AERONET}}$ (Levy et al., 2013). The expected error envelopes are used to evaluate the performance of MAIAC algorithm.

4. Validation results

4.1. Spatio-temporal collocation and overall comparison

Satellite aerosol measurements provide spatial coverage at a short time interval, while ground-based measurements provide high temporal resolution of aerosol information at local station. The validation procedure requires to calculate the spatiotemporal window of a collocated satellite and ground-based AOD pair (Martins et al., 2017; Superczynski et al., 2017; Tao et al., 2017; Gupta et al., 2018). We performed twenty

Table 1
Location in each AERONET stations.

ID	Station Name	Latitude	Longitude	Altitude(m)	ID	Station Name	Latitude	Longitude	Altitude(m)
1	Dunhuang	94.79	40.03	1381	27	Hangzhou_City	120.15	30.28	30
2	Yulin	109.71	38.28	1080	28	Shanghi_Minhang	121.39	31.13	49
3	Beijing	116.38	39.97	92	29	Zhongshan	113.38	22.51	39
4	XiangHe	116.96	39.75	36	30	Lanzhou_City	103.85	36.04	1516
5	Hefei	117.16	31.90	36	31	Mt_WLG	100.89	36.28	3816
6	Hong_Kong_PolyU	114.17	22.30	30	32	QOMS_CAS	86.94	28.36	4276
7	Taihu	120.21	31.42	20	33	Minqin	102.95	38.60	1373
8	BackGarden_GZ	113.02	23.29	16	34	Beijing_RADI	116.37	40.00	59
9	City_GZ	113.15	23.08	58	35	Litang	100.26	29.97	3930
10	Yufa_PEK	116.18	39.30	20	36	Muztagh_Ata	75.03	38.40	3674
11	PKU_PEK	116.18	39.59	66	37	Zhongshan_Univ	113.39	23.06	27
12	SACOL	104.13	35.94	1965.8	38	Dunhuang_LZU	94.95	40.49	1061
13	Xinglong	117.57	40.39	899	39	Beijing-CAMS	116.31	39.93	106
14	NAM_CO	90.96	30.77	4746	40	Hong_Kong_Sheung	114.11	22.48	40
15	Asia1	87.65	43.78	935.9	41	Shijiazhuang-SZF	114.45	38.01	71
16	Ningbo	121.54	29.85	37	42	AOE_Baotou	109.62	40.85	1314
17	Hangzhou-ZFU	119.72	30.25	42	43	XuZhou-CUMT	117.14	34.21	59.7
18	LA-TM	119.44	30.32	439	44	Lingshan_Mountain	115.49	40.05	1653
19	Qiandaohu	119.05	29.55	133	45	SONET_Harbin	126.6	45.70	187.9
20	Hong_Kong_Hok_Tsui	114.25	22.20	80	46	SONET_Hefei	117.16	31.90	36
21	NUIST	118.71	32.20	62	47	SONET_Nanjing	118.95	32.11	52
22	Shanghi_Met	121.54	31.22	5	48	SONET_Shanghai	121.48	31.28	24
23	Jingtai	104.1	37.33	1583	49	SONET_Xingtai	114.36	37.18	185.1
24	Kaiping	112.53	22.31	51	50	SONET_Zhoushan	122.18	29.99	29
25	Shouxian	116.78	32.55	22.7	51	Beijing_PKU	116.31	39.99	53
26	Zhangye	100.27	39.07	1461					

collocated data sets of AOD at 550 nm from both Terra and Aqua, matched with ground-based measurements. The collocated data sets contained five-time intervals from 10 to 120 min centered at Terra and Aqua transit time with four spatial windows from 3 km to 100 km centered at each AERONET station. Table 2 shows sample size and overall validation results of MAIAC AOD compared to AERONET measurements. The correlation coefficient varies from 0.91 to 0.925 with the RMSE of 0.192–0.199 for Aqua. The percentage of MAIAC AOD within the envelopes of EE is from 68.6% to 73.8%. The MAIAC AOD agrees well with the matched AETONET AOD under different time lags and spatial windows. The sample size increases with time lag. Due to the requirement of at least 40% of valid values in our study, the number of matchups might decrease with spatial window. For the window of 25 km, the sample size, percentage of MAIAC AOD within EE, and correlation coefficient are larger than those of 3 km window. Therefore, the window of 25 km is selected as the balance window in this study. For time interval of 60 min, the correlation coefficient is a little smaller than those within the time interval of 10 min and 30 min for Terra MAIAC AOD at the spatial window of 25 km. To comprise the sample size and correlation coefficient, the time interval of 60 min is selected. Collocated of AERONET AOD and MAIAC AOD are defined as the average of AERONET measurements within 60 min and MODIS observations within a sampling window of 25 km*25 km.

Fig. 2 shows the validation of MAIAC AOD against AERONET measurements over China. Blue line represents the 1:1 line and red line is the regression line. Black lines are the envelopes of EE. There are 8677 and 9450 MAIAC AOD observations matched with AERONET AOD measurements for Aqua and Terra, respectively. High correlation (0.924–0.933) are shown with RMSE of 0.187–0.193. There 72.4% of retrievals falling within the EE and 18.6% (9%) are overestimated (underestimated) for Aqua MAIAC AOD. For Terra MAIAC AOD, 74% of measurements are within the envelopes of EE and 19.7% (6.3%) are overestimated (underestimated). The slope of the regression line is close to 1 for Aqua and Terra. The analysis indicates that the MAIAC AOD performance very well over China. Fig. 3 illustrates the difference between MAIAC AOD and AERONET AOD against AERONET AOD. The result shows bias trend against AERONET AOD. The errors lead a relatively small positive bias when the AOD is lower than 0.1. When the AOD is greater than 0.3, the bias increases with the AOD magnitude. The result indicates that the uncertainties of MAIAC algorithm increase with the AOD magnitude.

4.2. Error dependencies

In this section, we investigate the relationship between MAIAC-AERONET measurements differences and sorts of parameters that could induce the aerosol retrieval errors. Aerosol Ångström Exponent (AE) represents the particle size and it can be used to understand the aerosol size impacts on MAIAC aerosol retrieval. Fig. 4 illustrates the MAIAC AOD bias as a function of AERONET AE. At low AOD (< 0.4), the bias increases with AERONET AE for both Aqua and Terra MAIAC AOD. Negative bias is shown at coarse particle size ($AE < 1$) and positive bias is presented when the AERONET AE is higher than 1. MAIAC retrievals for AOD higher than 0.4 also present same trend of bias. The absolute bias for high AOD condition is much larger than those for low AOD. The results indicate that MAIAC retrievals present negative bias of MAIAC AOD for coarse particles ($AE < 1$) and positive bias for mixed and small particles ($AE > 1$).

The surface reflectance and aerosol models vary with seasons over China. This could also influence the estimation of Aqua and Terra AOD. Therefore, the performance of MAIAC AOD is evaluated in different seasons. Fig. 5 and Fig. 6 present the scatterplots of AERONET measurements and MAIAC observations comparisons in spring, summer, autumn, and winter for Aqua and Terra, respectively. We collect more than 2200 samples in spring, autumn, and winter. Only about 1100 samples are selected in Summer due to the large impact of cloud. The MAIAC AOD agrees well with AERONET AOD in autumn and winter with high correlation (0.947 and 0.913) and RMSE (0.165 and 0.154). There are more than 75% of AOD falling within the envelopes of EE for Aqua and Terra in autumn and winter. The performance of MAIAC retrievals in summer is the worst with large RMSE (0.284) and there are more than 37% of AOD retrievals falling out of the EE envelopes. The result indicates that the AOD in summer is overestimated. Only about 62% of MAIAC AOD falls in the EE. In this study, we only pick the pixels under clear sky. Therefore, the influence of cloud on aerosol retrievals can be ignored. The large AOD bias in summer is related to the surface

Table 2
Analysis of various spatial and temporal window for MAIAC Aqua and Terra AOD (Number of matchups/correlation coefficient/RMSE/the percentage of matchups within the envelopes of EE/ > EE/ < EE).

		t ≤ 10 min	t ≤ 30 min	t ≤ 60 min	t ≤ 90 min	t ≤ 120 min
d ≤ 3 km	Aqua	7126/0.925/0.194/0.716/0.189/0.094	8058/0.922/0.196/0.712/0.192/0.097	8359/0.921/0.198/0.713/0.189/0.098	8532/0.921/0.199/0.712/0.188/0.099	8647/0.92/0.2/0.71/0.188/0.102
d ≤ 7 km		7234/0.925/0.195/0.72/0.191/0.089	8188/0.923/0.197/0.715/0.192/0.093	8505/0.923/0.198/0.714/0.19/0.096	8683/0.922/0.199/0.715/0.187/0.098	8796/0.921/0.2/0.711/0.187/0.101
d ≤ 25 km		7360/0.925/0.192/0.726/0.19/0.084	8350/0.923/0.194/0.723/0.189/0.088	8677/0.924/0.193/0.724/0.186/0.09	8864/0.925/0.192/0.724/0.185/0.091	8983/0.925/0.192/0.724/0.182/0.094
d ≤ 100 km		7267/0.911/0.199/0.687/0.212/0.102	8339/0.91/0.199/0.686/0.206/0.108	8731/0.912/0.197/0.69/0.204/0.105	8927/0.915/0.194/0.695/0.2/0.105	9050/09017/0.191/0.7/0.194/0.106
d ≤ 3 km	Terra	7771/0.934/0.184/0.738/0.205/0.057	8806/0.932/0.188/0.734/0.203/0.062	9163/0.929/0.193/0.734/0.2/0.065	9324/0.927/0.196/0.73/0.204/0.066	9451/0.925/0.198/0.727/0.205/0.068
d ≤ 7 km		7851/0.933/0.187/0.738/0.204/0.058	8903/0.932/0.189/0.733/0.204/0.062	9264/0.928/0.194/0.734/0.201/0.065	9423/0.927/0.197/0.731/0.203/0.067	9551/0.925/0.199/0.727/0.204/0.069
d ≤ 25 km		7961/0.935/0.183/0.741/0.202/0.058	9070/0.935/0.185/0.738/0.202/0.06	9450/0.933/0.187/0.74/0.197/0.063	9610/0.932/0.189/0.741/0.198/0.061	9742/0.931/0.191/0.737/0.2/0.063
d ≤ 100 km		7882/0.916/0.192/0.702/0.218/0.079	9079/0.916/0.194/0.703/0.214/0.082	9543/0.915/0.194/0.706/0.212/0.081	9730/0.916/0.194/0.71/0.21/0.08	9869/0.916/0.193/0.713/0.208/0.078

reflectance estimation because of the intercept of the regression line. In winter, the slope of the regression line is 0.847 and this means the background aerosol model used in the algorithm has large errors. In general, high accuracy of MAIAC AOD is shown in autumn, winter and MAIAC algorithm performs worst in summer for both Aqua and Terra.

Due to the spectral signature of different land covers, there are many methods to estimate the surface reflectance, such as the methods used in Dark Target (DT) and Deep Blue (DB) algorithm. DT algorithm calculates surface reflectance using a linear relationship between visible and shortwave infrared bands in vegetations regions (Kaufman et al., 1997), while DB algorithm adopts pre-calculated surface reflectance database (Hsu et al., 2013). These two algorithms can be applied to dense vegetation regions and bright surface. MAIAC algorithm uses time-series data to separate the contributions of surface reflectance and atmospheric aerosols (Lyapustin et al., 2011b, 2012). It also considers the surface bidirectional reflectance distribution function (BRDF) effects. There are three different surface types used in the DB algorithm (Hsu et al., 2013). In this study, some stations are located near the water. Therefore, four types of land cover are adopted to evaluate the performance of MAIAC AOD, including 1) arid and semiarid regions, 2) general vegetation, 3) urban/built-up and transitional regions, and 4) water (Hsu et al., 2013). Fig. 7 and Fig. 8 show the statistics of MAIAC retrievals and AERONET measurements in these four surface types. For water regions, MAIAC AOD from two sensors is high correlated with AERONET AOD, with correlation of ~0.919. However, there are more than 52% of measurements falling out the EE envelopes. The intercept and slope of regression line is 0.118 and 1.108. This indicates that both of surface reflectance estimation and aerosol model have large uncertainties in these regions. The correlation between MAIAC AOD and AERONET AOD in forest/grassland is 0.872 and 0.868 for Aqua and Terra, respectively. There are still more than 62% of AOD falling in the EE. The intercept and slope of the regression line in this surface type also show that the surface reflectance is overestimated and the aerosol model tends to underestimate the AOD. In urban/cropland regions, the MAIAC algorithm performs very well. The correlation is ~0.93 for both sensors and the RMSEs are 0.2 and 0.192 for Aqua and Terra, respectively. More than 77% of retrievals are within the EE. The surface reflectance estimation is very well and the slope of the regression line is also close to 1:1 line. In desert, the slope of the regression line is about 0.855 and it means the aerosol models used in MAIAC algorithm induce large errors. The surface reflectance estimation is very accurate. However, the sample size is very limited. Therefore, the performance in this region needs more studies. The MAIAC algorithm performs best in urban and cropland regions. In other regions, the performance of MAIAC AOD is influenced by surface reflectance estimation and aerosol model. The large errors of AOD retrievals over desert region are induced by aerosol model. In water and forest/grassland, both aerosol model and surface reflectance estimation influence the accuracy of MAIAC AOD. However, the optical properties of aerosol model overestimate the AOD over water region and the AOD underestimate over forest and grassland.

5. Discussions

In this study, we present a comprehensive study on evaluating the performance of MAIAC AOD. The performance of MAIAC AOD is very well. However, there are still some bias in different situations. According to the analysis, the MAIAC AOD bias increases with the AOD magnitude. The aerosol size also influences the AOD bias. Large AOD bias is shown for large and small particle matter due to the background aerosol model in MAIAC aerosol algorithm. Fixed aerosol models are used in MAIAC aerosol algorithm. Aerosol model and surface reflectance are two main factors that influences the accuracy of MAIAC AOD. The slope and intercept of regression line can be used to classify the influence of aerosol model and surface reflectance, respectively (Tao et al., 2015). Overestimation of surface reflectance will lead to

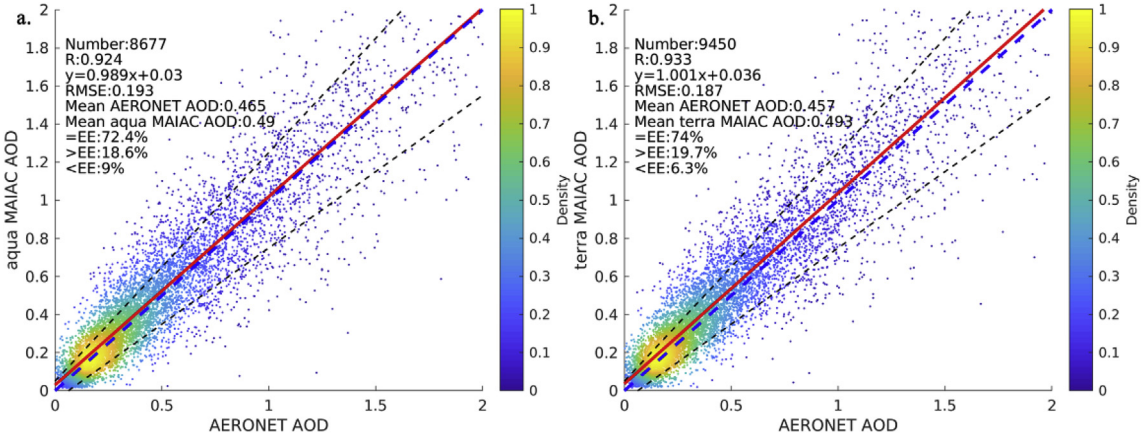

Fig. 2. Comparison between MAIAC AOD and AERONET measurements (a. Aqua, b. Terra).

more signals in top of apparent reflectance measurements be assigned to the effect of surface, hence less signal for AOD, in most condition, this means AOD will be underestimated. Overestimated AOD usually means underestimated surface. The surface reflectance estimation is more accurate in autumn than those in other three seasons. In winter, the bias of optical properties of aerosol induce largest bias in aerosol retrievals. The performance of MAIAC AOD in different surface types also has large differences. In arid and semiarid region, the aerosol model is the dominant factor of MAIAC AOD bias. In water and forest/grassland regions, both aerosol model and surface reflectance contribute to the AOD bias.

The MAIAC AOD is also evaluated over South America and United States. The MAIAC AOD generally shows high agreement with ground-based observations in these study regions. The MAIAC AOD also performs very well. According to the analysis in Martins et al. (2017), the bias between MAIAC retrieved AOD and AERONET measurements over South America is negative when the AOD is greater than 0.1. The negative bias in South America is induced by the biomass burning model in MAIAC algorithm. The analysis indicates that the MAIAC algorithm should improve the aerosol model by adopting the local aerosol optical properties. Consistent conclusion can be found in this study. The AOD bias is negative over United States, while the AOD bias is positive in China. This could also be influenced by the different aerosol optical properties in the study region.

The MAIAC AOD is also retrieved from MODIS. There are two aerosol products, including DB and DT AOD. Many studies are conducted to evaluate the performance of these two aerosol products by using the ground-based measurements over China. Fig. 9 shows the spatial distribution of correlation between MAIAC AOD and surface stations. The correlation is larger than 0.91 for Aqua and the correlation is larger than 0.92 for Terra in most of the stations. Lower correlation can be found in northwest China. The correlation of MODIS C6 10 km DT retrievals and different AERONET stations in east China is from 0.617 to 0.951 (Tao et al., 2015). Correlation between DB AOD and AERONET AOD is from 0.57 to 0.957. The analysis indicates that the correlation between MAIAC AOD and ground-based measurements is higher than those of MODIS aerosol products. Tao et al. (2017) found that the MODIS C6 DB aerosol products give a nearly-constant low values of 0.05 in desert regions due to the surface reflectance overestimation. According to our analysis in this paper, the surface reflectance estimation in MAIAC algorithm is relative accurate.

6. Conclusions

MODIS aerosol optical depth (AOD) are the most widely used aerosol products. Although the products have undergone several important improvements, there are still many uncertainties. Multiangle Implementation of Atmospheric Correction (MAIAC) algorithm was developed to improve the current MODIS data sets. The validation in China has not been conducted. In this study, Aqua and Terra at 1 km over China from MAIAC algorithm are obtained and evaluated against the ground-based AERONET measurements. The average of AERONET measurements within 60 min and MODIS observations within a sampling window of 25 km*25 km are collocated to compromise the sample size and correlation. Overall there are 8594 collocations of Aqua retrievals and 8851 collocations for Aqua.

The analysis indicates that surface reflectance and aerosol model used in MAIAC algorithm influence the accuracy of aerosol retrievals.

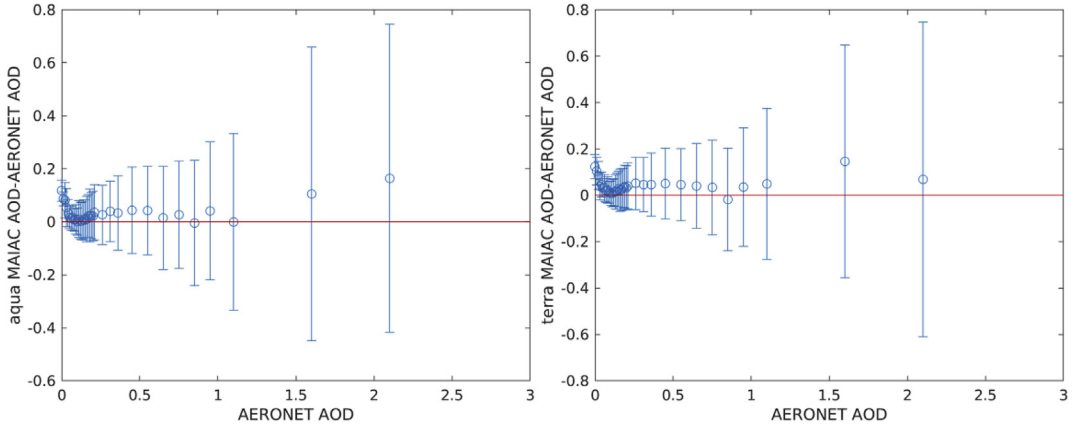

Fig. 3. The bias between MAIAC AOD and AERONET AOD against AERONET AOD (a. Aqua, b. Terra).

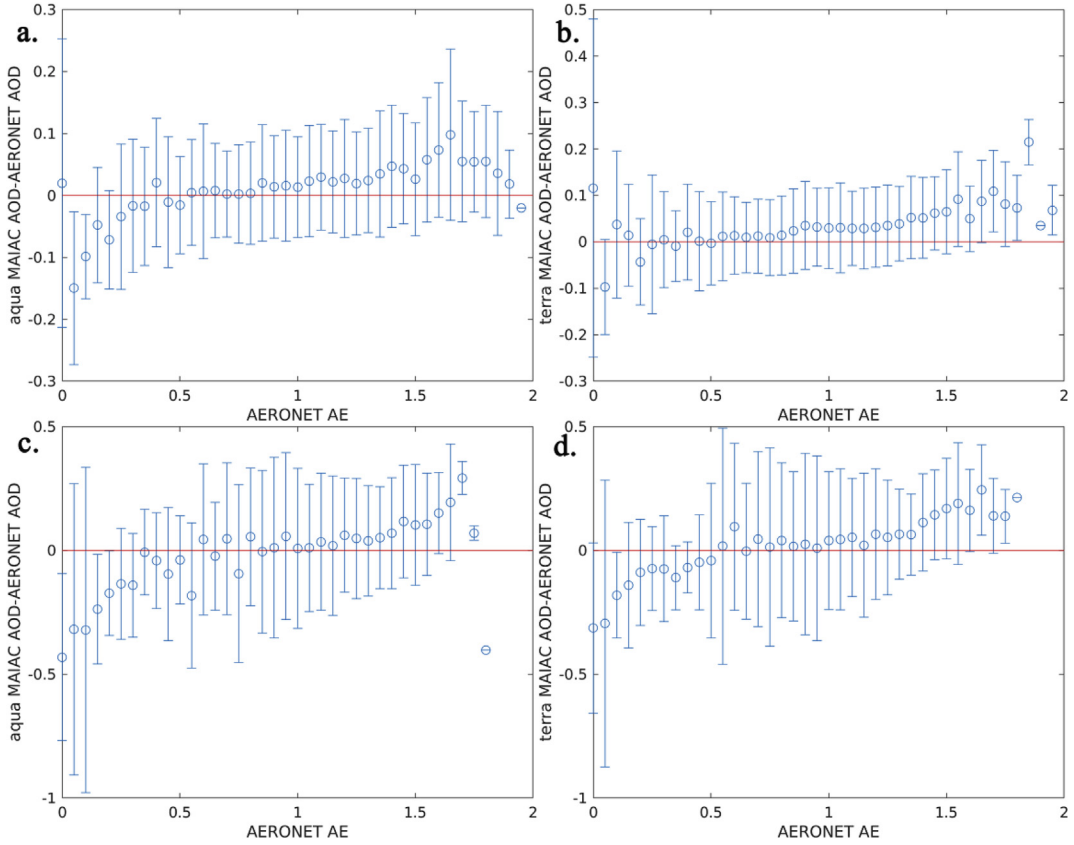

Fig. 4. The bias between MAIAC AOD and AERONET AOD against AERONET Ångström Exponent (a. Aqua AOD < 0.4, b. Terra AOD < 0.4, c. Aqua AOD > 0.4, d. Terra AOD > 0.4).

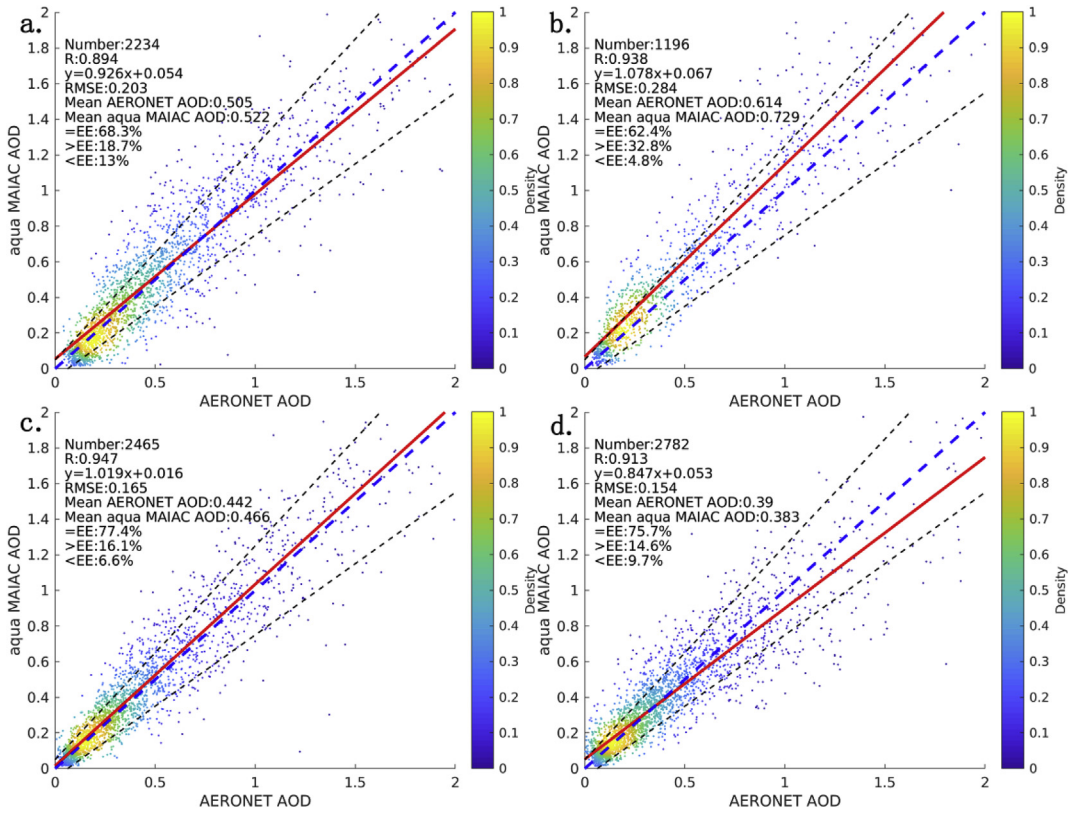

Fig. 5. The comparison of Aqua MAIAC AOD and AERONET AOD in a. spring, b. summer, c. autumn, and d. winter.

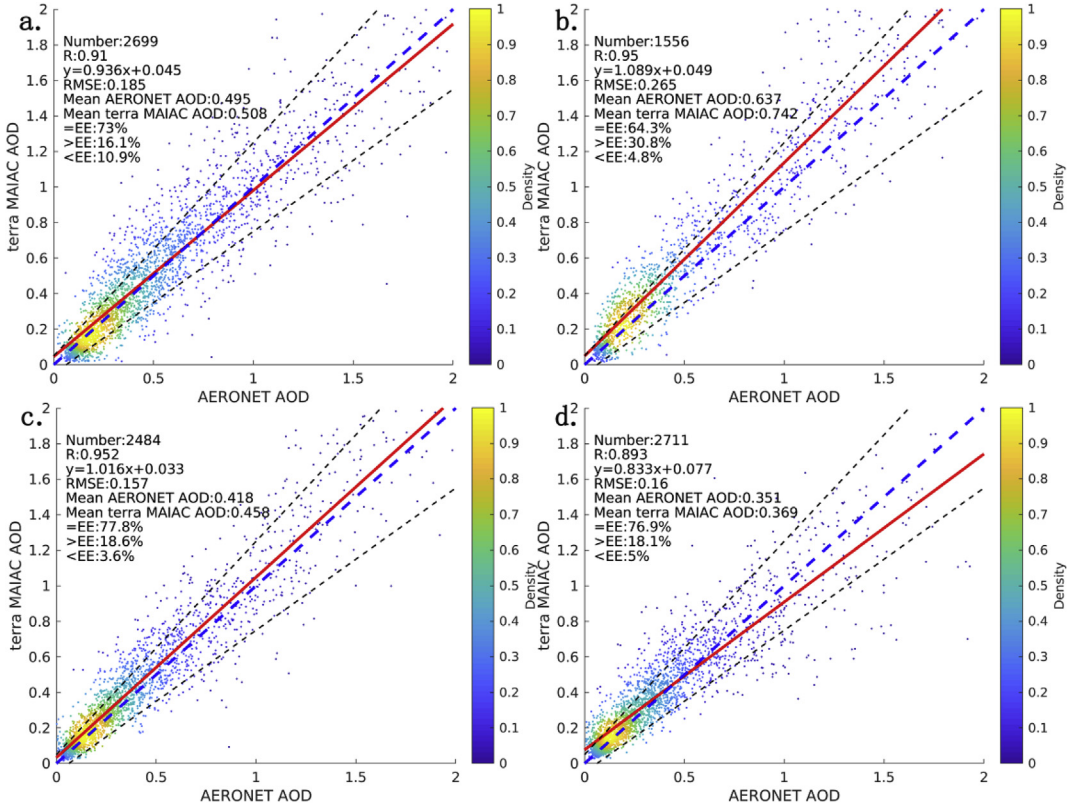

Fig. 6. The comparison of Terra MAIAC AOD and AERONET AOD in a. spring, b. summer, c. autumn, and d. winter.

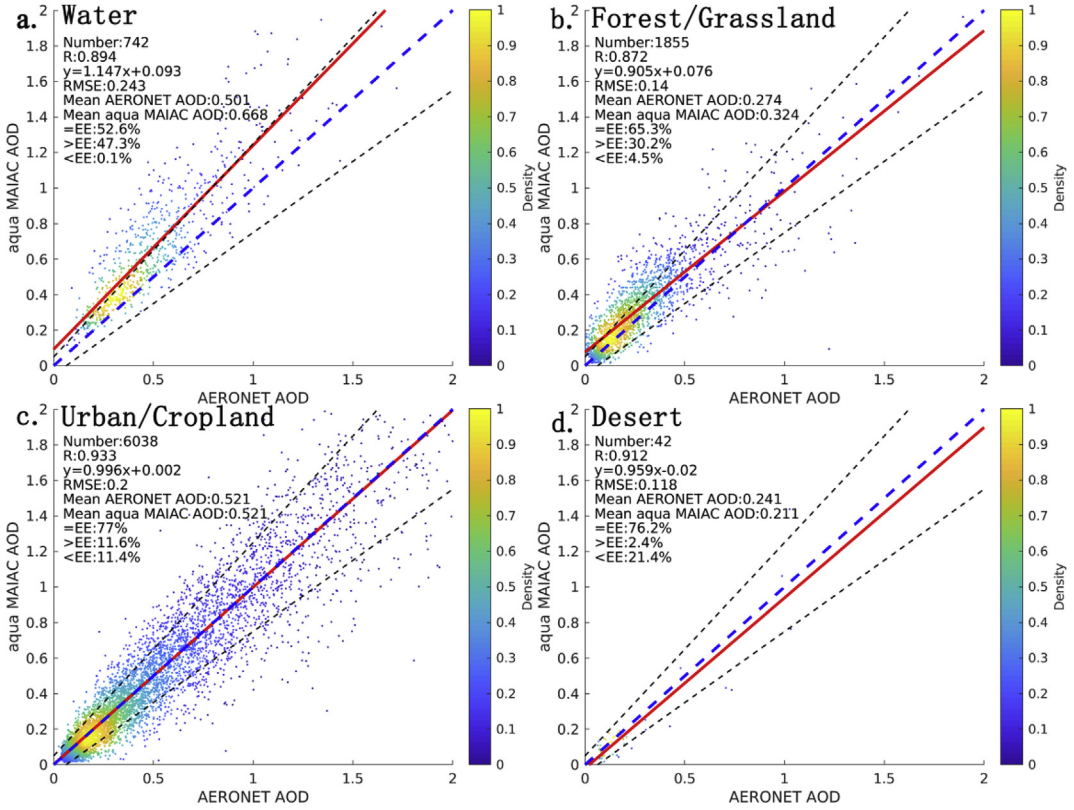

Fig. 7. The comparison of Aqua MAIAC AOD and AERONET AOD over different surface types.

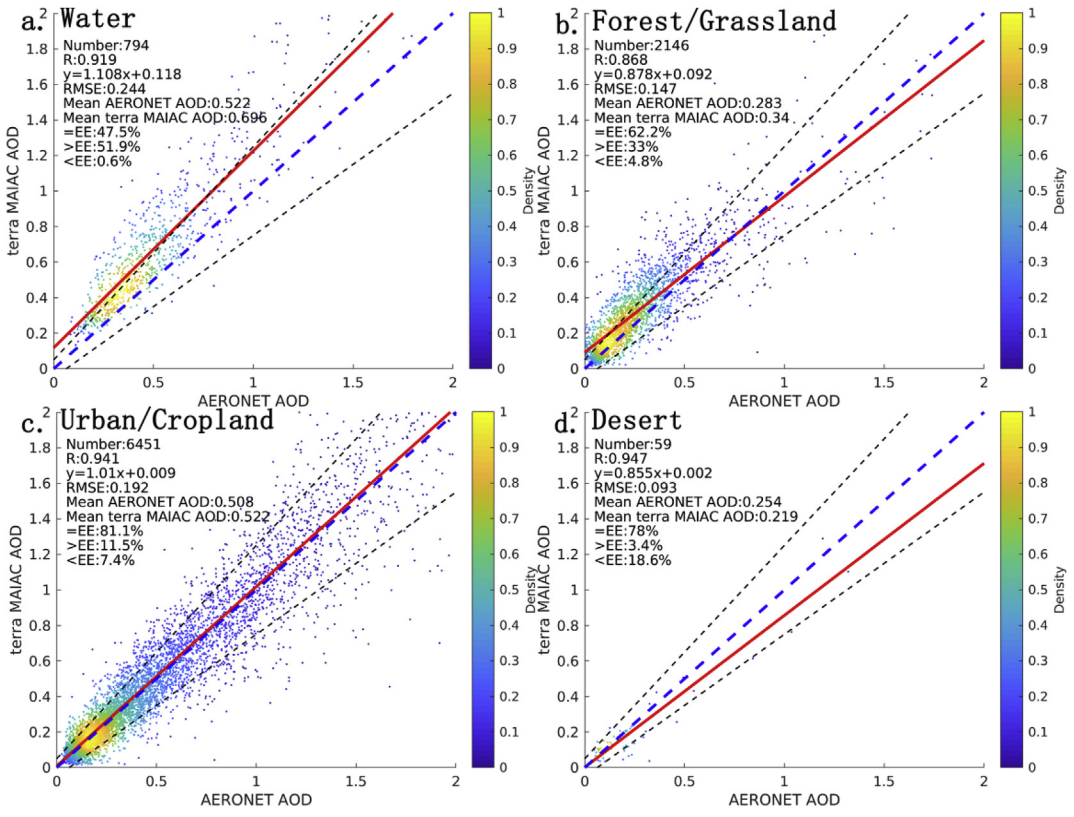

Fig. 8. The comparison of Terra MAIAC AOD and AERONET AOD over different surface types.

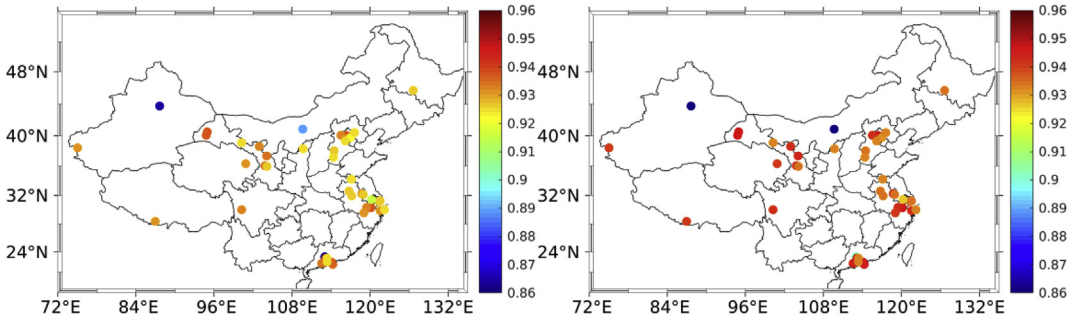

Fig. 9. The spatial distribution of correlation coefficient between MAIAC AOD and ground-based AOD (left: Aqua; right: Terra).

There are more than 72% of retrievals falling within the EE envelopes with high correlation (0.924 for Aqua and 0.933 for Terra). The analysis indicates that the MAIAC AOD has better performance than the existed MODIS aerosol products. The AOD bias is related to the AOD magnitude. Positive AOD bias is shown in China due to the impact of aerosol optical properties. The aerosol size also related to the bias of AOD. The background aerosol model is used in the algorithm. Therefore, AOD with large and small aerosol size has large AOD bias. MAIAC AOD is also analyzed as a function of seasons. Better performance of MAIAC retrievals are shown Autumn than those in other three seasons. We also investigate the MAIAC retrievals over different land cover types. The surface reflectance estimation has a large impact on the AOD retrievals over water region and it also influences the MAIAC AOD over forest/grassland. The large AOD bias in desert regions is mainly impacted by aerosol model. This study first comprehensively validates the 1 km MAIAC AOD over China. In all, the MAIAC AOD has a better performance than the existed MODIS AOD and it can be used to estimate the surface particle matters. However, the performance of MAIAC AOD in desert region are not fully evaluated due to the limited number of ground-based measurements. More study should be conducted in this region.

Conflicts of interest

The authors declare no conflict of interest.

Acknowledgements

This study was supported by the Zhejiang Provincial Natural Science Foundation of China (Grant No. LQ18D010004), National Science Foundation of China (Grant No. 41801258 and 41871254) and Open Fund of State Key Laboratory of Remote Sensing Science (Grant No. OFSLRSS201813). The authors would like to thank the team of AERONET for their hard work. We appreciate a large work of MODAPS team on MAIAC integration.

Appendix A. Supplementary data

Supplementary data to this article can be found online at https://doi.org/10.1016/j.atmosenv.2019.01.013.

References

Chew, B.N., Campbell, J.R., Reid, J.S., Giles, D.M., Welton, E.J., Salinas, S.V., Liew, S.C., 2011. Tropical cirrus cloud contamination in sun photometer data. Atmos. Environ. 45, 6724–6731.

Field, C.B., Barros, V.R., Mach, K., Mastrandrea, M., 2014. Climate change 2014: impacts, adaptation, and vulnerability. In: Working Group II Contribution to the IPCC 5th Assessment Report-Technical Summary, pp. 1–76.

Friedl, M.A., McIver, D.K., Hodges, J.C.F., Zhang, X.Y., Muchoney, D., Strahler, A.H., Woodcock, C.E., Gopal, S., Schneider, A., Cooper, A., Baccini, A., Gao, F., Schaaf, C., 2002. Global land cover mapping from MODIS: algorithms and early results. Rem. Sens. Environ. 83, 287–302.

Ghotbi, S., Sotoudeheian, S., Arhami, M., 2016. Estimating urban ground-level PM10 using MODIS 3km AOD product and meteorological parameters from WRF model. Atmos. Environ. 141, 333–346.

Gupta, P., Remer, L.A., Levy, R.C., Mattoo, S., 2018. Validation of MODIS 3 km land aerosol optical depth from NASA's EOS Terra and Aqua missions. Atmos. Meas. Tech. 11, 3145–3159.

Hinds, W.C., 1999. Aerosol Technology: Properties. Behavior, and Measurement of Airborne Particles (2nd).

Holben, B.N., Eck, T.F., Slutsker, I., Tanre, D., Buis, J.P., Setzer, A., Vermote, E., Reagan, J.A., Kaufman, Y.J., Nakajima, T., Lavenu, F., Jankowiak, I., Smirnov, A., 1998. AERONET - a federated instrument network and data archive for aerosol characterization. Rem. Sens. Environ. 66, 1–16.

Hsu, N.C., Jeong, M.J., Bettenhausen, C., Sayer, A.M., Hansell, R., Seftor, C.S., Huang, J., Tsay, S.C., 2013. Enhanced Deep Blue aerosol retrieval algorithm: the second generation. J. Geophys. Res.: Atmosphere 118, 9296–9315.

Ichoku, C., Kaufman, Y.J., Remer, L.A., Levy, R., 2004. Global aerosol remote sensing from MODIS. Adv. Space Res. 34, 820–827.

Kaufman, Y.J., Wald, A.E., Remer, L.A., Gao, B.C., Li, R.R., Flynn, L., 1997. The MODIS 2.1-mu m channel - correlation with visible reflectance for use in remote sensing of aerosol. Ieee T Geosci. Rem. 35, 1286–1298.

Levy, R.C., Mattoo, S., Munchak, L.A., Remer, L.A., Sayer, A.M., Patadia, F., Hsu, N.C., 2013. The Collection 6 MODIS aerosol products over land and ocean. Atmos. Meas. Tech. 6, 2989–3034.

Levy, R.C., Mattoo, S., Sawyer, V., Shi, Y., Colarco, P.R., Lyapustin, A.I., Wang, Y., Remer, L.A., 2018. Exploring systematic offsets between aerosol products from the two MODIS sensors. Atmos. Meas. Tech. 11, 4073–4092.

Levy, R.C., Remer, L.A., Kleidman, R.G., Mattoo, S., Ichoku, C., Kahn, R., Eck, T.F., 2010. Global evaluation of the Collection 5 MODIS dark-target aerosol products over land. Atmos. Chem. Phys. 10, 10399–10420.

Li, S.S., Chen, L., Zheng, F., Han, D., Wang, Z., 2009. Design and application of haze optic thickness retrieval model for Beijing olympic games. In: Geoscience and Remote Sensing Symposium,2009. IEEE International,IGARSS pp. II-507-II-510.

Li, X., Zhang, C., Li, W., Liu, K., 2017. Evaluating the use of DMSP/OLS nighttime light imagery in predicting PM2.5 concentrations in the northeastern United States. Rem. Sens-Basel 9, 620.

Li, Z., Lau, W.K.M., Ramanathan, V., Wu, G., Ding, Y., Manoj, M.G., Liu, J., Qian, Y., Li, J., Zhou, T., Fan, J., Rosenfeld, D., Ming, Y., Wang, Y., Huang, J., Wang, B., Xu, X., Lee, S.S., Cribb, M., Zhang, F., Yang, X., Zhao, C., Takemura, T., Wang, K., Xia, X., Yin, Y., Zhang, H., Guo, J., Zhai, P.M., Sugimoto, N., Babu, S.S., Brasseur, G.P., 2016. Aerosol and monsoon climate interactions over Asia. Rev. Geophys. 54, 866–929.

Li, Z.Q., Xu, H., Li, K.T., Li, D.H., Xie, Y.S., Li, L., Zhang, Y., Gu, X.F., Zhao, W., Tian, Q.J., Deng, R.R., Su, X.L., Huang, B., Qiao, Y.L., Cui, W.Y., Hu, Y., Gong, C.L., Wang, Y.Q., Wang, X.F., Wang, J.P., Du, W.B., Pan, Z.Q., Li, Z.Z., Bu, D., 2018. Comprehensive study of optical, physical, chemical, and radiative properties of total columnar atmospheric aerosols over China: an overview of sun–sky radiometer observation network (SONET) measurements. Bull. Am. Meteorol. Soc. 99, 739–755.

Lin, C.Q., Li, Y., Lau, A.K.H., Deng, X.J., Tse, T.K.T., Fung, J.C.H., Li, C.C., Li, Z.Y., Lu, X.C., Zhang, X.G., Yu, Q.W., 2016. Estimation of long-term population exposure to PM2.5 for dense urban areas using 1-km MODIS data. Rem. Sens. Environ. 179, 13–22.

Lyapustin, A., Martonchik, J., Wang, Y.J., Laszlo, I., Korkin, S., 2011a. Multiangle implementation of atmospheric correction (MAIAC): 1. Radiative transfer basis and look-up tables. J. Geophys. Res. Atmos. 116, 1–9.

Lyapustin, A., Wang, Y., Korkin, S., Huang, D., 2018. MODIS Collection 6 MAIAC algorithm. Atmos. Meas. Tech. 11, 5741–5765.

Lyapustin, A., Wang, Y., Laszlo, I., Kahn, R., Korkin, S., Remer, L., Levy, R., Reid, J.S., 2011b. Multiangle implementation of atmospheric correction (MAIAC): 2. Aerosol algorithm. J. Geophys. Res. Atmos. 116, 1–15.

Lyapustin, A.I., Wang, Y., Laszlo, I., Hilker, T., Hall, F.G., Sellers, P.J., Tucker, C.J., Korkin, S.V., 2012. Multi-angle implementation of atmospheric correction for MODIS (MAIAC): 3. Atmospheric correction. Rem. Sens. Environ. 127, 385–393.

Malm, W.C., Molenar, J.V., Eldred, R.A., Sisler, J.F., 1996. Examining the relationship among atmospheric aerosols and light scattering and extinction in the Grand Canyon area. J. Geophys. Res. 101 19,251-219,265.

Martins, V.S., Lyapustin, A., de Carvalho, L.A.S., Barbosa, C.C.F., Novo, E.M.L.M., 2017. Validation of high-resolution MAIAC aerosol product over South America. J. Geophys. Res. Atmos. 122, 7537–7559.

Ramanathan, V., Feng, Y., 2009. Air pollution, greenhouse gases and climate change: global and regional perspectives. Atmos. Environ. 43, 37–50.

Remer, L.A., Mattoo, S., Levy, R.C., Munchak, L.A., 2013. MODIS 3 km aerosol product: algorithm and global perspective. Atmos. Meas. Tech. 6, 1829–1844.

Superczynski, S.D., Kondragunta, S., Lyapustin, A.I., 2017. Evaluation of the multi-angle implementation of atmospheric correction (MAIAC) aerosol algorithm through intercomparison with VIIRS aerosol products and AERONET. J. Geophys. Res.: Atmosphere 122, 3005–3022 2016JD025720.

Tao, M., Chen, L., Wang, Z., Wang, J., Che, H., Xu, X., Wang, W., Tao, J., Zhu, H., Hou, C., 2017. Evaluation of MODIS Deep Blue aerosol algorithm in desert region of east Asia: ground validation and intercomparison. J. Geophys. Res.: Atmosphere 122 10,357-310,368.

Tao, M.H., Chen, L.F., Wang, Z.F., Tao, J.H., Che, H.Z., Wang, X.H., Wang, Y., 2015. Comparison and evaluation of the MODIS Collection 6 aerosol data in China. J. Geophys. Res. Atmos. 120, 6992–7005.

Wang, Z.F., Chen, L.F., Tao, J.H., Zhang, Y., Su, L., 2010. Satellite-based estimation of regional particulate matter (PM) in Beijing using vertical-and-RH correcting method. Rem. Sens. Environ. 114, 50–63.

Wei, J., Sun, L., Huang, B., Bilal, M., Zhang, Z., Wang, L., 2018. Verification, improvement and application of aerosol optical depths in China Part 1: inter-comparison of NPP-VIIRS and Aqua-MODIS. Atmos. Environ. 175, 221–233.

Yassaa, N., 2016. Air pollution may alter efforts to mitigate climate change. Atmos. Environ. 127, 221–222.

Zhang, Z., Fan, M., Wu, W., Wang, Z., Tao, M., Wei, J., Wang, Q., 2019a. A simplified aerosol retrieval algorithm for Himawari-8 advanced Himawari imager over Beijing. Atmos. Environ. 199, 127–135.

Zhang, Z., Wu, W., Fan, M., Tao, M., Wei, J., Jin, J., Tan, Y., Wang, Q., 2019b. Validation of Himawari-8 aerosol optical depth retrievals over China. Atmos. Environ. 199, 32–44.

Zhang, Z., Wu, W., Wei, J., Song, Y., Yan, X., Zhu, L., Wang, Q., 2017. Aerosol optical depth retrieval from visibility in China during 1973–2014. Atmos. Environ. 171, 38–48.

Zhang, Z.Y., Wong, M.S., 2017. A simplified method for retrieving aerosol optical thickness using visibility data between 1980 and 2014, a case study in China. Ieee J-Stars 10, 4409–4416.

Zhang, Z.Y., Wong, M.S., Campbell, J.R., 2018. Conceptualizing How Severe Haze Events Are Impacting Long-Term Satellite-Based Trend Studies of Aerosol Optical Thickness over Asia. Springer, Cham.

Zhang, Z.Y., Wong, M.S., Lee, K.H., 2015. Estimation of potential source regions of PM2.5 in Beijing using backward trajectories. Atmos. Poll. Res. 6, 173–177.

Zhang, Z.Y., Wong, M.S., Lee, K.H., 2016a. Evaluation of the representativeness of ground-based visibility for analysing the spatial and temporal variability of aerosol optical thickness in China. Atmos. Environ. 147, 31–45.

Zhang, Z.Y., Wong, M.S., Nichol, J., 2016b. Global trends of aerosol optical thickness using the ensemble empirical mode decomposition method. Int. J. Climatol. 36, 4358–4372.

Zhong, S., Qian, Y., Zhao, C., Leung, R., Wang, H., Yang, B., Fan, J., Yan, H., Yang, X.-Q., Liu, D., 2016. Urbanization-induced urban heat island and aerosol effects on climate extremes in the Yangtze River Delta Region of China. Atmos. Chem. Phys. Discuss. 2016, 1–57.

Zhuang, B.L., Li, S., Wang, T.J., Deng, J.J., Xie, M., Yin, C.Q., Zhu, J.L., 2013. Direct radiative forcing and climate effects of anthropogenic aerosols with different mixing states over China. Atmos. Environ. 79, 349–361.